

# Palaeoclimatic implications of the magnetic record from loess/palaeosol sequence Viatovo (NE Bulgaria)

Diana Jordanova,<sup>1</sup> Jozef Hus<sup>2</sup> and Raoul Geeraerts<sup>2</sup>

<sup>1</sup>Geophysical Institute, Bulgarian Academy of Sciences, Acad. G. Bonchev Str., bl.3, 1113 Sofia, Bulgaria. E-mail: vanedi@geophys.bas.bg

<sup>2</sup>Centre de Physique du Globe, Dourbes, Belgium

Accepted 2007 August 2. Received 2007 August 2; in original form 2007 January 22

## SUMMARY

Loess-palaeosol deposits in the lower Danube area represent the southeastern edge of the loess cover in Europe. Detailed rock magnetic investigations of the loess/palaeosol sequence in Viatovo in NE Bulgaria reveal that magnetite and maghemite of very fine superparamagnetic grain size are responsible for the magnetic enhancement of palaeosol units. A detailed palaeoclimatic record is obtained through high-resolution measurements of magnetic susceptibility, frequency dependent magnetic susceptibility and CaCO<sub>3</sub> content. Magnetic proxies indicate a more warm and humid climate during the development of the older palaeosol units (S<sub>4</sub>–S<sub>6</sub>).

**Key words:** Bulgaria, loess, magnetite, maghemite, palaeosol, rock magnetism.

## 1 INTRODUCTION

The widespread loess-palaeosol sequences in the temperate climatic belt are amongst the most important geological terrestrial palaeoclimatic records. They consist of alternating loess and palaeosol horizons, corresponding, respectively, to cold glacial and warm interglacial conditions. Establishing chronologies of loess sequences and their stratigraphic correlation with deep-sea sediments are, therefore, important topics for reconstruction of the Earth's history during the Quaternary (Maher & Thompson 1992; Maher *et al.* 1994; Heller and Evans 1995; Ding *et al.* 2002; Sun & An 2004). In the absence of unambiguous biomarkers and difficulties in their dating, magnetopalaeoclimatology and palaeomagnetic dating of loess sediments are important tools for establishing the loess stratigraphy and for environmental reconstructions.

The palaeoclimatic significance of the magnetic climate proxies (e.g. magnetic susceptibility, anhysteretic remanence, various ratios of magnetic parameters) have been discussed in the context of the role of dust sources, climate, and other time-related factors for the magnetic enhancement of palaeosol units (e.g. Maher 1998; Harrison *et al.* 2001; Liu *et al.* 2004; Deng *et al.* 2005; Qiu *et al.* 2005). To better understand the role of global, regional and local palaeoenvironmental conditions leading to the formation and properties of the loess-palaeosol deposits, data from different geographical areas are needed. Studies of loess sediments from the lower Danube area may contribute to deciphering the global picture of palaeoclimatic conditions during the Quaternary. The main goal of the present study is to reveal regional palaeoclimate development in southeastern Europe.

## 2 GEOLOGICAL DESCRIPTION

The Viatovo section is located in Northeastern Bulgaria, at the southern edge of the Danube plain, about 30 km southeast of Russe

(Fig. 1), at an altitude of 200–230 m above sea level. Loess deposits and underlying red clays rest on the Pliocene denudation surface (PDS), developed in karstic Lower Cretaceous limestones with palaeokarsts that are infilled with kaolin (Evlogiev 1993). The Viatovo section is exposed in a quarry that was opened for extraction of kaolin. The complete sedimentary sequence on the PDS above the kaolinitic level is represented in this region by red clays and a loess/palaeosol sequence consisting of eight loess horizons and seven palaeosols (Evlogiev 2006). However, loess accumulation in the area south of Russe (e.g. Viatovo quarry) was relatively weak and resulted in deposits of reduced thickness and higher degree of pedogenic alterations compared to loess/palaeosol deposits situated close to the Danube river (Jordanova & Petersen 1999a,b). This is the reason why only six palaeosols and seven loess horizons are discriminated at Viatovo.

## 3 SAMPLING AND METHODS

The complete loess/palaeosol sequence at Viatovo has been sampled in four non-overlapping sections, following the natural boundaries between loesses and palaeosols. Section 1 includes: topsoil S<sub>0</sub>, first loess unit L<sub>1</sub>, first palaeosol unit S<sub>1</sub> and units L<sub>2</sub>, S<sub>2</sub> and L<sub>3</sub>. Section 2 covers palaeosol units S<sub>3</sub> and S<sub>4</sub> with a thin CaCO<sub>3</sub> layer in between (probably the remnant of L<sub>4</sub>), units L<sub>5</sub>, S<sub>5</sub> and L<sub>6</sub>. Section 3 is represented by palaeosol S<sub>6</sub> and the underlying loess unit L<sub>7</sub>. The fourth section cuts 5.60 m through the red clays, down to the kaolin level. The total thickness of the complete composite section is 27 m.

To establish a high-resolution magnetic susceptibility stratigraphy, 540 loose samples were taken at a sampling interval of 5 cm. Some of the samples collected at 10 cm intervals were used for geochemical analyses—organic content, total CaCO<sub>3</sub> content and grain size analysis. Rock magnetic investigations including



**Figure 1.** Location of the Viatovo section, and the other studied loess-palaeosol sections in the region.

thermomagnetic analysis of magnetic susceptibility and hysteresis measurements were carried out on loose samples.

Hysteresis measurements of 35 loose samples, from representative levels of the profile, and thermal  $M_i(T)$  analysis were performed in a Variable Field Translation Balance (VFTB) in a maximum field of 500 mT. Bulk and frequency-dependent low field magnetic susceptibility of the loose samples was measured using a Bartington MS2 magnetic susceptibility meter. Another set of hysteresis measurements was carried out in a translation inductometer in a maximum field of 1 T. High-temperature susceptibility behaviour [ $K(T)$ ] was studied using the CS-3 oven of a KLY-3 Kappabridge for identification of the magnetic mineralogy.

Four magnetically enriched separates of two samples from  $S_1$  and  $L_2$  were prepared using a Frantz Isodynamic separator at currents of 0.1 A ( $\sim 0.15$  T field) (strongly magnetic fractions SM) and 1.0 A [weak magnetic fractions WM ( $\sim 1$  T field)] for Mössbauer spectroscopy carried out in the Department of Subatomic and Radiation Physics at the University of Gent.

Geochemical analyses were carried out on 124 loose samples. Grain size analysis was done using the areometer method. The total carbon content was determined in a 'Shaibler' apparatus, which operates on the basis of the detection of released  $\text{CO}_2$  upon reaction of the sample with HCl. The organic content was determined by the method of Turin (1937).

## 4 EXPERIMENTAL RESULTS

### 4.1 Magnetic susceptibility, frequency dependence of susceptibility and geochemical analyses

A high-resolution (5 cm interval) low-field bulk magnetic susceptibility profile was obtained for the Viatovo section. Variations of

mass-specific magnetic susceptibility ( $\chi$ ) along the profile (Fig. 2) discriminate the magnetically enhanced palaeosol horizons from the underlying parent loesses. The first three palaeosol units— $S_1$ ,  $S_2$  and  $S_3$ —are characterized by as much as five times higher maximum  $\chi$  values, in comparison with the less-weathered loess. Below  $L_5$ , the magnetic susceptibility contrast between the soil and loess layers is reduced, suggesting that pedogenesis has also affected the loess layers. Well-expressed susceptibility variations in the red clays (21–27 m depth) suggest that they also probably represent a pedo-complex of superimposed palaeosols. The same conclusions can be drawn on the basis of the per cent frequency dependent magnetic susceptibility [ $\chi_{FD}$  per cent =  $(\chi_{LF} - \chi_{HF}) \times 100/\chi_{LF}$ ], used as an indicator for the presence of ultrafine superparamagnetic (SP) grains (Maher 1986; Heller *et al.* 1991; Forster *et al.* 1994; Dearing *et al.* 1997). Relatively high values, up to 12 per cent, are observed in the palaeosol units and the red clay. The presence of significant secondary magnetic enhancement can be deduced from the high  $\chi_{FD}$  per cent values in the first loess unit  $L_1$ , as well as in units  $L_3$ ,  $L_4$  and  $L_7$  (Fig. 2).

Grain size analysis, calcium carbonate content ( $\text{CaCO}_3$ ) and organic content determinations were made on 124 samples. The most clearly expressed differences among the values of the measured parameters for loess and palaeosol samples are found for the  $\text{CaCO}_3$  content. It reaches values  $>20$  per cent in the loess units, showing an inverse relationship with magnetic susceptibility (Fig. 2). Organic content (humus) varies from 0.1 to 0.88 per cent with maximum values attained in the topsoil. Organic content may be influenced by other factors (e.g. bioturbation, destruction with age) which blur the significance of this parameter as a proxy for the past environment. Clay content, determined here as  $d < 0.005$  mm according to the Bulgarian national standard, does not vary significantly. The mean clay content, both in loess and soil horizons, is around 30 per cent. Exceptions are loess units  $L_2$  and  $L_5$ , where lower

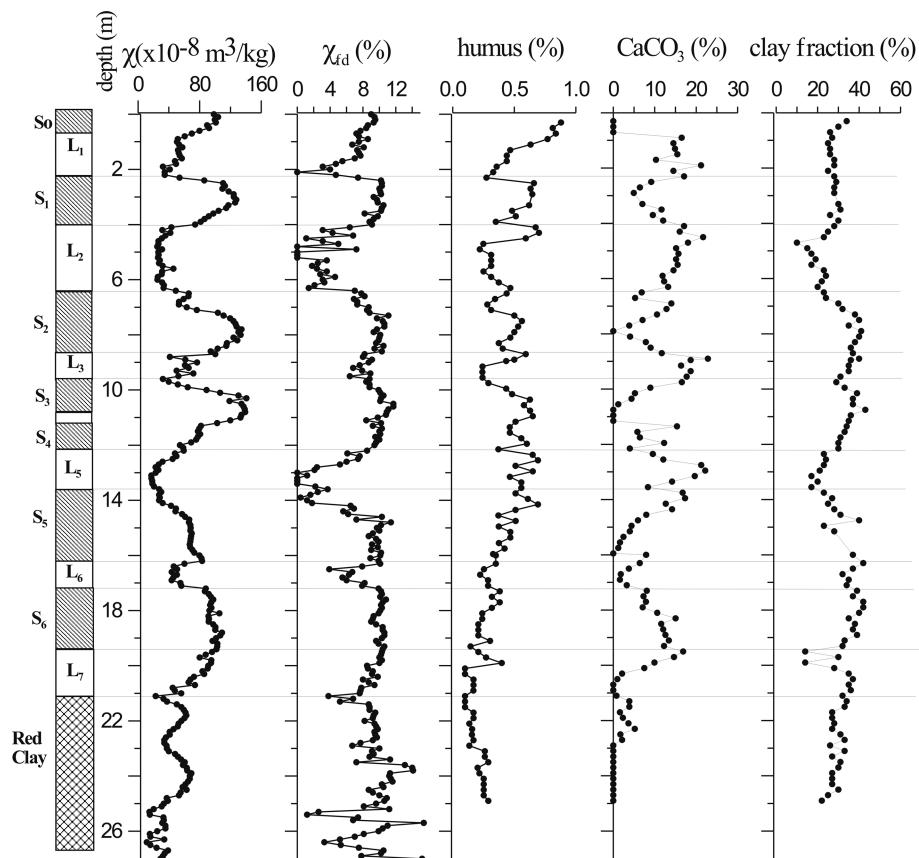


**Figure 2.** Depth variations of low-field magnetic susceptibility, percent frequency dependent susceptibility, humus, calcium carbonate ( $\text{CaCO}_3$ ) and clay content at Viatovo.

values are observed. The observed small differences in clay content are probably a manifestation of the enhanced weathering and pedogenesis, even during the glacials, particularly in the lower part of the section.

Frequency-dependent susceptibility measurements were further used to infer the background susceptibility values using the approach of Forster *et al.* (1994). In contrast to previous studies, the background susceptibilities were calculated for each unit separately and compared to the value obtained by using the whole data set. This approach was chosen based on the assumption that the grain size of the dust source material also changes according to climate, which would result in different background susceptibilities in the different units. The reliability of the calculated background susceptibility values for each unit  $\chi_{\text{bg}}$  was evaluated by the  $R^2$  of the regression line (Table 1). Fig. 3 shows the link between the calculated  $\chi_{\text{bg}}$  and the corresponding minimum susceptibility measured for each loess unit and the maximum susceptibility for each palaeosol unit. Three different linear relationships between the calculated background susceptibilities and the corresponding minimum/maximum enhancement of loess/palaeosol units are observed, dividing the palaeosols from the upper part of the section ( $S_1$ ,  $S_2$  and  $S_3$ ) from the older ( $S_4$ – $S_6$ ) plus  $S_0$  and red clays. Loesses except  $L_3$  form separate group. Further insight into the origin of magnetic enhancement is obtained by the relationship between magnetic susceptibility, its frequency dependent component and the relative contribution of the clay fraction, determined from the grain size analysis. A positive correlation is observed between low-field susceptibility ( $\chi_{\text{LF}}$ ), frequency dependent susceptibility ( $\chi_{\text{FD}}$ ) and the fine fraction ( $d < 5 \mu\text{m}$ ) (Fig. 4).

**Table 1.** Calculated background susceptibilities ( $\chi_{\text{bg}}$ ) separately for each loess and palaeosol unit (first column) with its coefficient of determination  $R^2$  (second column) and the absolute values of the maximum ( $\chi_{\text{max}}$ ) susceptibility of palaeosol units or minimum ( $\chi_{\text{min}}$ ) susceptibility of loess units (third column).

Unit	$\chi_{\text{bg}}$ ( $10^{-8} \text{ m}^3 \text{ kg}^{-1}$ )	$R^2$	$\chi_{\text{max soil}}/\chi_{\text{min loess}}$ ( $10^{-8} \text{ m}^3 \text{ kg}^{-1}$ )
$S_0$	29.0	0.975	103.9
$L_1$	25.8	0.849	32.3
$S_1$	14.1	0.919	127.6
$L_2$	22.6	0.900	25.2
$S_2$	18.6	0.826	134.3
$L_3$	3.4	0.958	32.2
$S_3$	22.7	0.900	140.7
$S_4$	21.5	0.963	80.6
$L_5$	19.1	0.915	17.3
$S_5$	14.0	0.775	83.1
$L_6$	29.1	0.854	43.6
$S_6$	25.3	0.801	109.0
$L_7$	16.0	0.957	22.9
Red clay 1	11.8	0.825	69.2
Red clay 2	7.6	0.878	38.9
Whole profile	15.8	0.940	

#### 4.2 Magnetic mineralogy

Thermomagnetic analyses of susceptibility ( $K$ ) and induced magnetization ( $M_i$ ) with increasing temperature up to  $700 \text{ }^\circ\text{C}$  (in air) were carried out for identification of the main ferrimagnetic phases

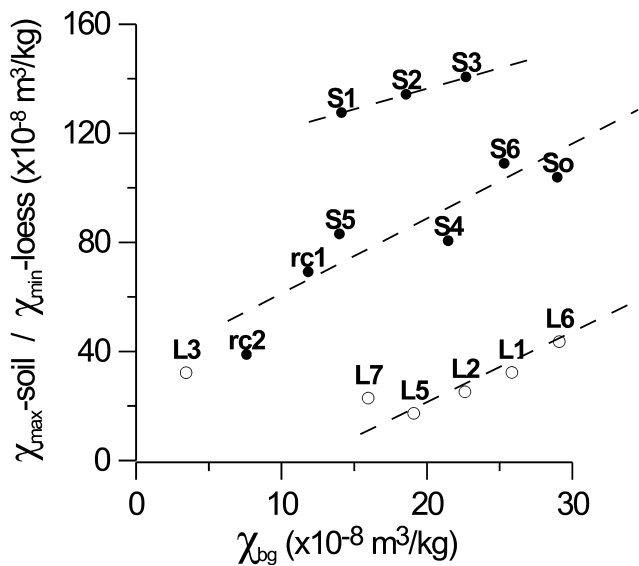


**Figure 3.** Relationship between the calculated background magnetic susceptibilities ( $\chi_{bg}$ ) in different loess and soil units of the Viatovo section and the corresponding minimum (for loesses) and maximum (for palaeosols) susceptibility values found within the separate units. The abbreviations rc1 and rc2 refer to the two red clay units, which can be discriminated by their susceptibilities (see Fig. 2).

present in the loess/soil sediments of the Viatovo section. Representative examples of the thermal behaviour of magnetic susceptibility,  $K(T)$  are shown in Fig. 5a. All the samples exhibit similar  $K(T)$  curves, characterized by an initial smooth increase up to 200 °C, followed by a gradual decrease that is interrupted by a slight increase at 300–310 °C (which is more pronounced for the loess samples). The final Curie temperature ( $T_c$ ) of 580 °C and occasionally a small fraction with  $T_c \sim 620$  °C (not in the examples illustrated) are typical for all the heating curves. The cooling curve was always above the heating curve, suggesting the production of ferrimagnetic material during heating (Fig. 5a).

Thermomagnetic analysis of induced magnetization ( $M_i$ ) of the loess (weakly magnetic) and soil (strongly magnetic) samples were obtained in different inducing fields of, respectively, 45 and 21 mT, corresponding to the maximum fields that could be attained in the two VFTBs used for the measurements. Generally, two types of  $M_i(T)$  curves occur: (1) In the case of soil samples, where a higher inducing field (45 mT) was applied, a gradual decrease from room temperature up to 200 °C is evident, followed by a steeper, almost linear decrease up to 600 °C. The cooling curve is almost linear, showing either increase or decrease

of the  $M_i$  value at 80 °C (Fig. 5b). (2) Loess samples, measured in a lower field of 21 mT show a clear convex shape of the heating curve with a smooth decrease from 200 °C up to a final  $T_c$  of 600 °C (Fig. 5b). All the loess samples exhibit an increase of  $M_i$  on cooling.

Additionally, thermal behaviour of magnetic susceptibility,  $K(T)$ , of magnetic separates [strongly magnetic (SM) and weakly magnetic (WM) fractions] and bulk material from the  $S_1/L_2$  palaeosol/loess couplet was monitored (Fig. 6). The  $K(T)$  curves of the bulk soil sample (Fig. 6a) indicates a final  $T_c$  of 580 °C on the heating curve and subsequently a strong increase of susceptibility on cooling. This increase is caused by thermal transformations as seen in the  $K(T)$  behaviour of its WM fraction (Fig. 6e). The SM fractions show evidence of  $T_{cs}$  of 600 °C, which are also preserved in the cooling curves (Figs 6c and d). The  $K(T)$  curve of the bulk material of loess sample  $L_2$  exhibits the same shape as that of all other loess samples subjected to  $K(T)$  experiment (Fig. 6b). The SM fraction of  $L_2$  shows similar behaviour to the SM fraction of  $S_1$ . The only difference is that the effect of initial (up to 200 °C)  $K$ -increase is more pronounced. Similar to the case for SM fraction of  $S_1$ ,  $T_{cs}$  of 580 and 600 °C are evident.

Mössbauer absorption spectra at room temperature (RT) for the strongly magnetic (SM) and weakly magnetic (WM) fractions of the  $S_1/L_2$  couplet were obtained using a  $^{57}\text{Co}$  source. Results are given in Table 2 and the absorption spectra for  $L_2$  are shown in Fig. 7. The data presented in Table 2 suggest that both loess unit  $L_2$  and the palaeosol  $S_1$  have a similar magnetic mineralogy, with magnetite, oxidized magnetite and hematite being the principal magnetic minerals. The presence of maghemite was revealed in the strong magnetic fraction of  $S_1$  but not in  $L_2$ .

### 4.3 Magnetic grain size

Hysteresis parameters of 36 samples from all the units were obtained measuring hysteresis loops in two VFTB instruments with maximum applied fields of 200 and 500 mT. Although such fields can only saturate the magnetically soft fraction (e.g. magnetite), coercivity variations [coercive force ( $B_c$ ) and coercivity of remanence ( $B_{cr}$ )] show a good relationship with the lithology with higher values in the loess units (mainly in the upper part of the complex) and lower values in the palaeosol units (Fig. 8). Older loess horizons are obviously significantly influenced by secondary pedogenic (weathering) processes, resulting in lower coercivities due to the presence of pedogenic ultrafine magnetite grains. Concentration-dependent saturation magnetization ( $M_s$ ) and saturation remanence ( $M_{rs}$ ) exhibit systematically higher values in the palaeosols.

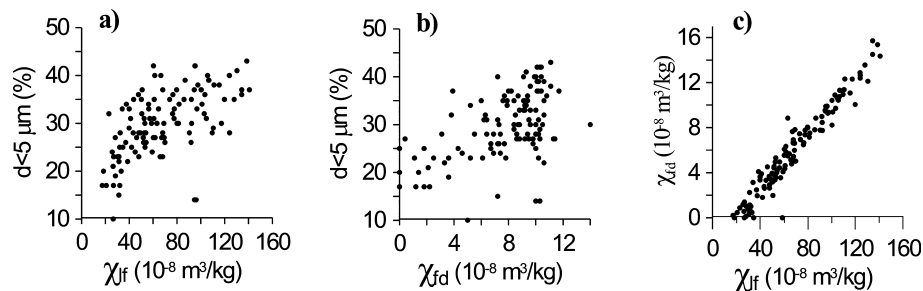


**Figure 4.** (a) Low field magnetic susceptibility ( $\chi_{LF}$ ) as a function of the fine (clay) fraction  $d < 5 \mu\text{m}$ ; (b) Frequency dependent susceptibility ( $\chi_{FD}$ ) as a function of the fine (clay) fraction  $d < 5 \mu\text{m}$  and (c) ( $\chi_{FD}$ ) as a function of the low field ( $\chi_{LF}$ ) magnetic susceptibility.

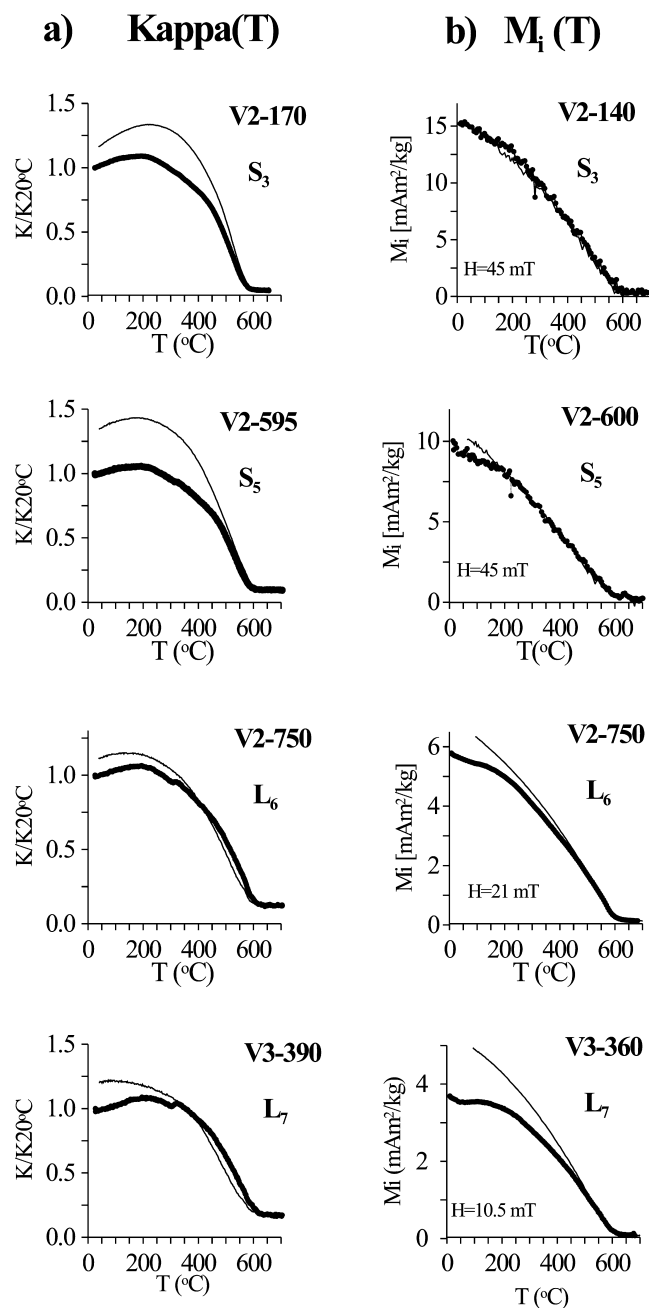


**Figure 5.** Thermomagnetic analysis: (a) examples of typical  $K(T)$  curves obtained in an Ar atmosphere; (b) examples of  $M_i(T)$  analysis in air. Heating curves denoted by solid circles, cooling curves—by thin line.

## 5 DISCUSSION

### 5.1 Magnetic mineralogy

The magnetic mineralogy of loess/palaeosol sediments has received considerable attention (Maher & Thompson 1992; Eyre & Shaw 1994; Heller & Evans 1995; Deng *et al.* 2004; Liu *et al.* 2004; Chen *et al.* 2005). The origin of the magnetic carriers in loesses and palaeosols is of major importance for the palaeoclimatic interpretation of loess magnetic properties and for magnetostratigraphical results (for a review, see Heller & Evans 1995).

Strong evidence for the dominant role of magnetite in the determination of  $K(T)$  behaviour is the observed  $T_c$  of 580 °C in all

the samples studied. Mineral transformations during heating above 300 °C, as can be seen in Fig. 6a, result in complex  $K(T)$  behaviour, which may reflect  $Fe_3O_4$  formation, detected in the heating curves. The shape and behaviour of induced magnetization curves [ $M_i(T)$ ] with increasing temperature (Fig. 5b) does not indicate any appearance of a new magnetic phase during heating. This apparent contradiction can be explained by the very different heating rates used in the two experiments. A single  $M_i(T)$  heating/cooling cycle is completed in about 25–30 min, or a rate of  $\sim 45$  °C  $min^{-1}$ , while  $K(T)$  curves were measured at a heating rate of 12 °C  $min^{-1}$ . All the  $K(T)$  and  $M_i(T)$  runs suggest similar magnetic mineralogy of the loess and palaeosol units, dominated by magnetite. Some degree of low-temperature oxidation (maghemitization) can be deduced from the relatively higher  $T_c$ 's of 600–620 °C on  $M_i(T)$  curves (Fig. 5b) and  $K(T)$  behaviour of strongly magnetic fractions of the samples from  $S_1/L_2$  couplet (Fig. 6), as shown also by the data from Mössbauer spectroscopy (Table 2). Hematite, detected by the latter method, does not make a significant contribution to the magnetic signal evidenced neither by the  $K(T)$ , nor by the  $M_i(T)$  experiments. Reasons for this may be its weak saturation magnetization (O'Reilly 1984; Dunlop & Ozdemir 1997) and perhaps also its poor crystallinity. Several possible causes for the increase in  $K$  after heating can be considered:

- (i) Thermal transformation of ferrihydrite to  $Fe_3O_4/\gamma-Fe_2O_3$  in the presence of organic matter (Cornell & Schwertmann 1996; Campbell *et al.* 1997).
- (ii) Formation of  $Fe_3O_4$  due to the thermal destruction of paramagnetic minerals (e.g. phyllosilicates, lepidocrocite), which results in liberation of  $Fe^{2+}$  ions from their crystal lattices (Ozdemir & Dunlop 1993; Gehring & Hofmeister 1994; Murad & Wagner 1998).
- (iii) Reduction of weakly magnetic antiferromagnetic phases present ( $\alpha-Fe_2O_3$ ) to  $Fe_3O_4$  (Cornell & Schwertmann 1996; Mullins 1977).

The observed magnetic susceptibility changes are most pronounced in the loess samples compared to the soil samples, suggesting that the possible source (among those, listed above), and/or the most favourable micro-environmental conditions, should be inherent to the parent material. Subsequent pedogenic processes would only bring about relative changes in the proportion of the newly created magnetic phase to the total signal or reaction conditions. Significant pedogenic alterations of the loess units in the Viatovo section, as deduced from the high values of  $\chi_{FD}$  per cent (Fig. 2), suggest that even less intense pedogenesis (e.g. in loesses) may lead to an increased amount of magnetic minerals, which transform into strongly magnetic  $Fe_3O_4$  upon heating to temperatures higher than 300 °C.

A more straightforward interpretation of the experimental results is provided by the results from the thermomagnetic analysis of magnetic susceptibility of the  $S_1/L_2$  couplet carried out on strongly magnetic (SM) and weakly magnetic (WM) fractions. As seen from Fig. 6, the significant increase of susceptibility in soil samples is due to thermal transformations in the WM fraction. It is characterized by significantly higher amounts of paramagnetic or superparamagnetic minerals at room temperature, as can be judged from the higher relative areas (RA per cent) of the doublets in the Mössbauer spectra, assigned to  $Fe^{3+}$  and  $Fe^{2+}$  in silicates and Fe-oxyhydroxides (Table 2). Mineralogical studies of Bulgarian loess (Minkov 1968) showed that the main phyllosilicate is illite in the loess and montmorillonite in the palaeosols. The SM fraction of soil unit  $S_1$  shows a decrease after heating, probably as a result of oxidation of the magnetite phase to hematite or to progressive maghemitization.

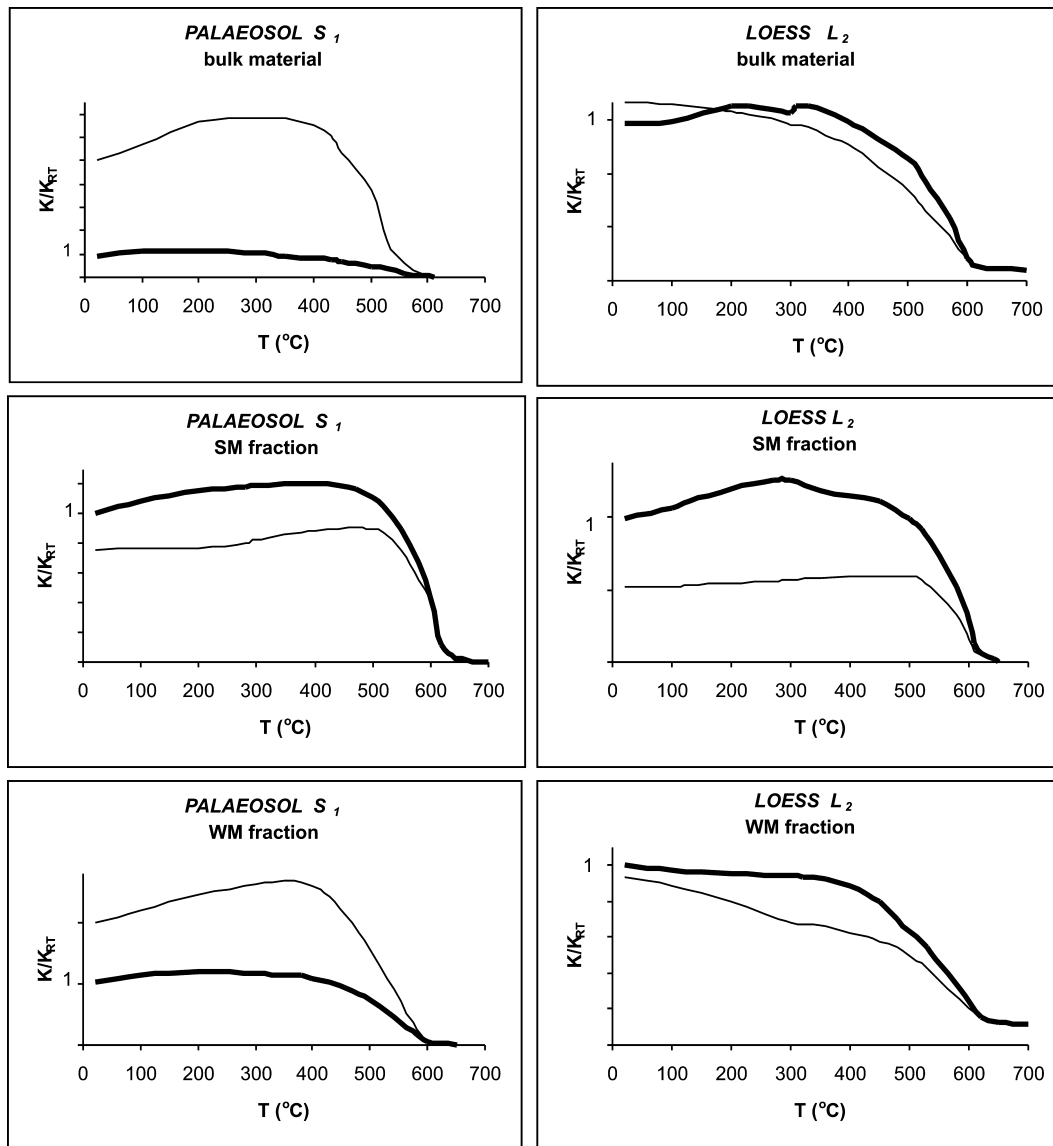


**Figure 6.** Thermomagnetic analyses of magnetic susceptibility  $K(T)$  for the  $S_1/L_2$  couplet: (a) bulk material of  $S_1$ , (b) bulk material of  $L_2$ , (c) strongly magnetic (SM) fraction of  $S_1$ , (d) strongly magnetic (SM) fraction of  $L_2$ , (e) weakly magnetic (WM) fraction of  $S_1$  and (f) weakly magnetic (WM) fraction of  $L_2$ . Susceptibility is normalized to the initial value at room temperature (RT). Heating curves denoted by solid circles, cooling curves by thin lines.

**Table 2.** Results from the Mössbauer analysis of SM and WM fractions of samples from the  $S_1/L_2$  couplet—measurements at room temperature (RT).

Sample	Palaeosol $S_1$				Assignment	Loess $L_2$			
	$H_{hf}$ (T)	$2\varepsilon$ or $\Delta$ ( $\text{mm s}^{-1}$ )	$\delta_{Fe}$ ( $\text{mm s}^{-1}$ )	RA (per cent)		$H_{hf}$ (T)	$2\varepsilon$ or $\Delta$ ( $\text{mm s}^{-1}$ )	$\delta_{Fe}$ ( $\text{mm s}^{-1}$ )	RA (per cent)
SM	51.2	-0.19	0.37	18	Hematite WF	51.4	-0.17	0.37	15
	48.9	0	0.29	19	Magnetite $\text{Fe}^{3+}$	49.1	0	0.27	29
	46.0	0	0.61	9	Magnetite $\text{Fe}^{2.5+}$	45.8	0	0.64	26
	40.0	0	0.34	11	Maghemite	-	-	-	-
	-	0.71	0.38	18	Silicate $\text{Fe}^{3+}$ and Fe-oxide	-	0.66	0.24	13
	-	0.72	0.93	12	Silicate $\text{Fe}^{n+?}$	-	0.69	0.95	10
	-	2.53	1.05	7	Silicate $\text{Fe}^{2+}$	-	2.36	1.24	3
	-	3.54	1.18	7	Garnet	-	3.52	1.30	5
WM	50.0	-0.19	0.37	10	Hematite WF	-0.20	0.37	7	
	-	0.77	0.32	43	Silicate $\text{Fe}^{3+}$ and Fe-oxide	0.80	0.34	46	
	-	1.16	0.78	12	Silicate $\text{Fe}^{n+?}$	1.19	0.74	10	
	-	2.70	1.09	25	Silicate $\text{Fe}^{2+}$	2.67	1.10	31	
	-	3.61	1.25	10	Garnet	3.61	1.25	6	

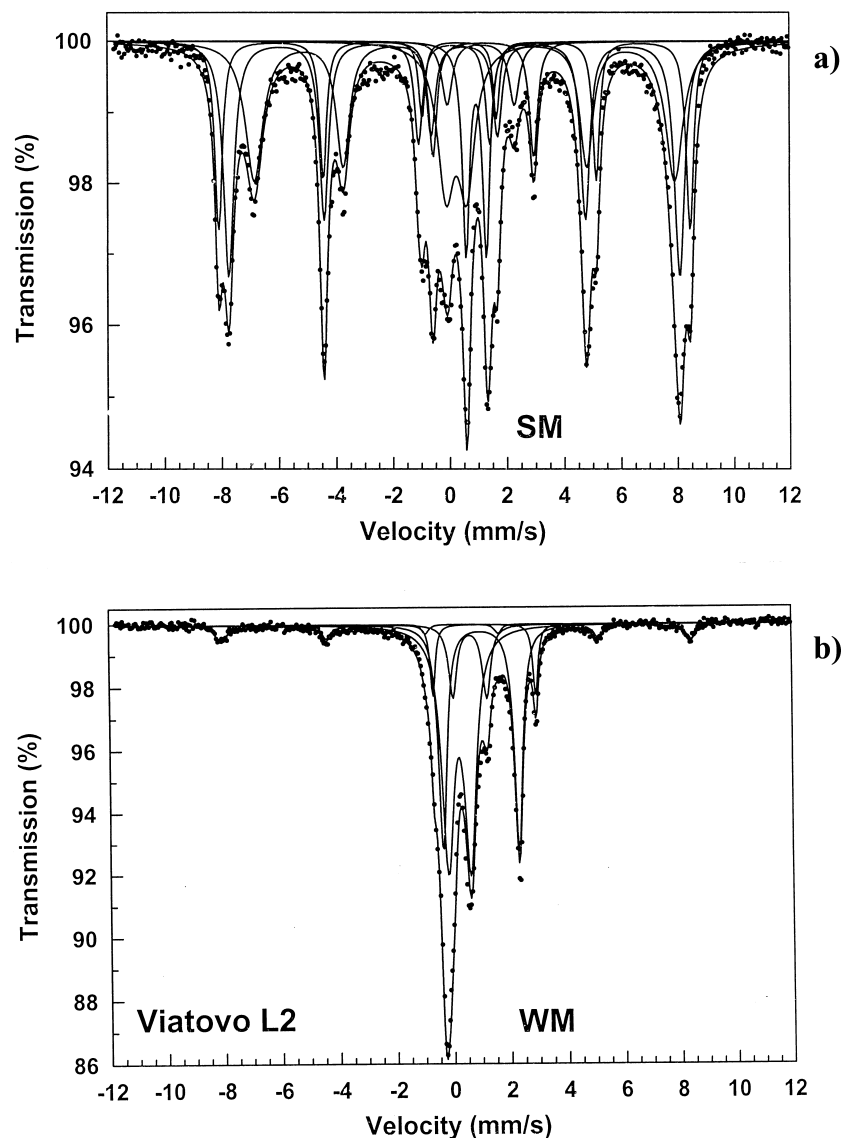


Figure 7. Room temperature (RT) Mössbauer spectra of a sample from loess unit L<sub>2</sub> (a) SM fraction and (b) WM fraction.

Therefore, several transformations can take place during heating to moderate temperatures in loess and soil samples:

(1) Dehydroxylation (loss of structural hydroxyl) at 300 °C, accompanied by oxidation of structural Fe<sup>2+</sup> to Fe<sup>3+</sup>, as confirmed by Mössbauer spectroscopy of illite (Murad & Wagner 1998), paralleling the first colour changes from yellowish towards reddish-brown.

(2) Combustion of humic and fulvic acids, taking place in the interval 300–550 °C (Weaver 1989).

(3) Thermal transformation of 6-line ferrihydrite to magnetite/maghemite in the presence of reductants (e.g. carbon source) upon heating above 300 °C (Campbell *et al.* 1997). The latter has been observed both in air and N<sub>2</sub>-atmospheres for a 1–20 per cent weight content of charcoal or glucose. In the absence of reductants, the direct transformation ferrihydrite–hematite is observed.

(4) Transformations of ferrimagnetic phases, initially present in the material like partial (surface) oxidation, crystal growth, release of internal stress (Van Velzen & Dekkers 1999).

A likely hypothesis in weathering environments is the formation of ferrihydrite, as it forms by rapid hydrolysis of an Fe<sup>3+</sup> salt solution

in the presence of small amounts of silicate (Cornell & Schwertmann 1996). The same reactions characterize the processes of chemical weathering and formation of clay minerals (Weaver 1989), during the formation of primary loess dust material. The presence of ferrihydrite is difficult to confirm because of its very small grain size (3–5 nm) and poor crystallinity (Vandenberghe *et al.* 1990; Goodman 1994; Murad 1998). As a metastable phase, 2-line ferrihydrite transforms to goethite or hematite, depending on temperature, pH, water activity and foreign compounds (Cornell & Schwertmann 1996). Its essential preservation in loess is favoured by the retarding role of organic ligands and Si in solution. On the other hand, favourable conditions for magnetite/maghemite synthesis, with ferrihydrite as a precursor, occur during pedogenesis (Schwertmann 1988; Maher 1998). As a result, the initial ferrihydrite quantity is consumed during the process of magnetite/ maghemite authigenesis. Laboratory heatings of loess and soil samples result generally in a significant increase of magnetic susceptibility at 300 °C in loesses but only a small increase in palaeosols, that will become more pronounced at higher temperatures ( $T > 450$  °C). A possible explanation, therefore, is that the ferrihydrite–magnetite/maghemite

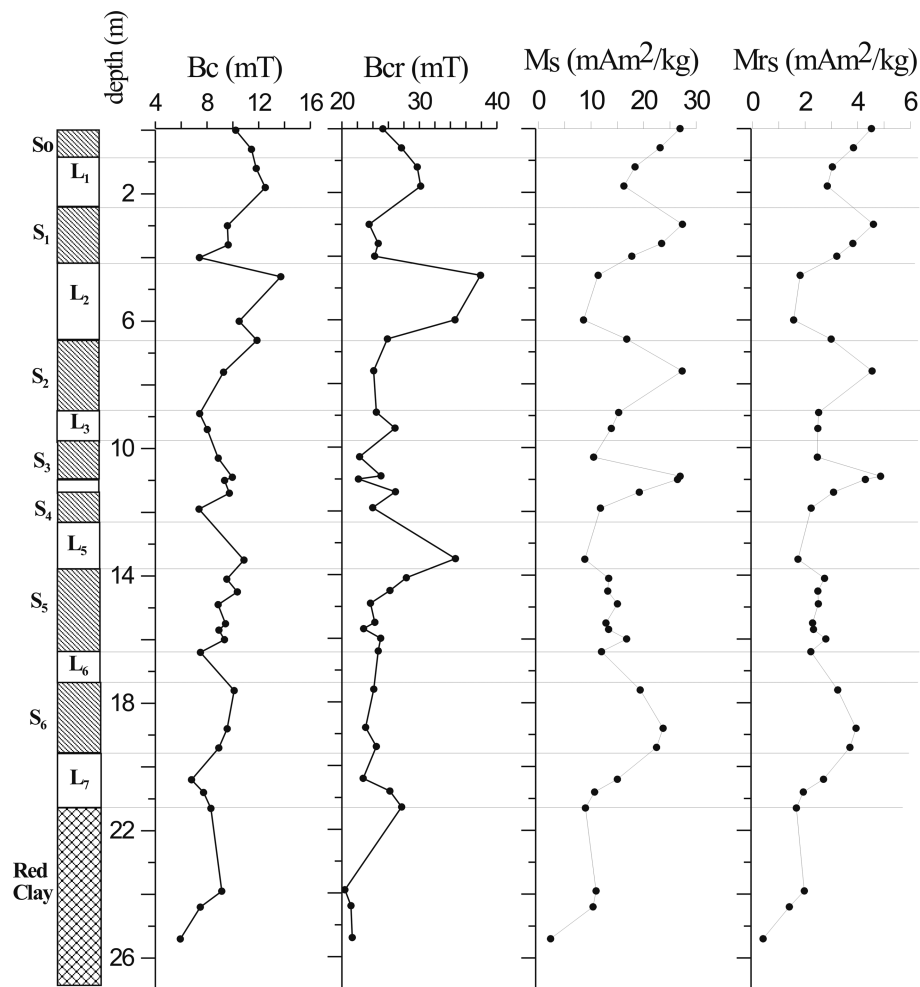


**Figure 8.** Variations of the coercivity parameters  $B_c$  and  $B_{cr}$ , saturation magnetization ( $M_s$ ) and saturation remanence ( $M_{rs}$ ) with depth in the Viatovo section.

transformation takes place in weathered loess samples because of the presence of some organic material (Campbell *et al.* 1997), as is suggested also by the observed variations in humus content in the Viatovo section (Fig. 2). As was experimentally observed (Campbell *et al.* 1997), the ferrihydrite–magnetite/maghemite transformation, starting at 300 °C, is probably related to the temperature at which humus combustion starts.

The reactions described above depend also on the duration of heating (Cornell & Schwertmann 1996), which explains the observed differences in relative changes in the magnetic parameters  $M_i$  and magnetic susceptibility, being most pronounced after longer heating times.

## 5.2 Palaeoenvironmental reconstructions

Thermomagnetic analyses suggest that variations of magnetic susceptibility  $\chi$  along the Viatovo profile are mainly controlled by concentration changes of the strongly magnetic fraction. The observed clear contrast between the loess and palaeosol units (Fig. 2) is similar to the one observed in other loess/palaeosol sequences in China, Central Asia and Europe (Maher & Thompson 1995; Oches & Banerjee 1996; Forster & Heller 1997). Site-specific peculiarities in concentration and grain size variations can give valuable information about the role of local climate conditions, relief, vegetation,

parent material, as far as these factors determine soil formation (Jenny 1941). The presence of authigenic ultrafine SP magnetites as a result of pedogenesis (Zhou *et al.* 1990; Maher & Thompson 1992) can be easily identified by measuring the frequency-dependent magnetic susceptibility  $\chi_{FD}$  per cent (Maher 1988; Heller *et al.* 1991; Dearing *et al.* 1997). As shown in Fig. 2, all the palaeosol units are characterized by high  $\chi_{FD}$  per cent values, up to 12 per cent, pointing to a significant SP fraction as high as 80 per cent, according to the phenomenological model of Dearing *et al.* (1997). A relatively high content of SP  $Fe_3O_4$  grains can also be assumed for loess units  $L_1$ ,  $L_3$ ,  $L_6$ ,  $L_7$ , as  $\chi_{FD}$  per cent reaches here values of 8–9 per cent (Fig. 2). The presence of pedogenic, magnetically soft grains in the SP and viscous SP/SD state in loesses is also supported by the relatively low coercivity ( $B_c$  and  $B_{cr}$ ) values in these units (Fig. 8), comparable to the palaeosols. The high  $\chi_{FD}$  per cent values in the red clays may reflect the presence of SP hematite grains with high Al-substitution (Wells *et al.* 1999), which is a common phenomenon for weathering environments (Schwertmann 1988; Cornell & Schwertmann 1996). The question remains whether the magnetic enhancement of the loess units containing SP grains is caused by secondary alteration of the dust material as a result of pedogenesis, or by weathering of the primary detrital fraction in the source area. Fig. 3 shows the dependence between the calculated background susceptibility ( $\chi_{bg}$ ) per unit and the corresponding maximum ( $\chi_{max}$ ) or minimum ( $\chi_{min}$ ) susceptibility values. An exception is loess unit  $L_3$

(Fig. 3), which shows a very low  $\chi_{bg}$  together with relatively high  $\chi_{min}$  values among loess units. The latter is probably an indication that the whole thickness of this loess unit was significantly influenced by secondary pedogenic alteration, after deposition. On the other hand, the rest of the loess units (with the possible exception of L<sub>7</sub>) follow the well-determined linear trend (Fig. 3). This can be explained in terms of a varying content and grain size of 'primary' windblown (detrital) ferrimagnetic grains within the loess units. The distribution of the data points for soil horizons in Fig. 3 follow a less consistent trend, which can be explained by several possible factors. The major factor is the soil type, reflecting certain combinations of pedoenvironmental conditions (temperature, moisture, pH, illuviation, etc.) (Jenny 1941). The first three palaeosols, S<sub>1</sub>, S<sub>2</sub> and S<sub>3</sub>, which are considered to be of Chernozem type, logically form a single trend line, in contrast to the older palaeosols (S<sub>4</sub>, S<sub>5</sub> and S<sub>6</sub>), which are reddish in colour and display features of forest soils. However, another factor that may explain the deviations is erosion of the uppermost soil levels, where the highest magnetic enhancement occurs. This supposition confirms the field observations that S<sub>0</sub> is very thin Chernozem-like soil (the main soil type for the topsoil in the area), while S<sub>4</sub> and S<sub>3</sub> form a pedocomplex with only a thin CaCO<sub>3</sub> layer in between. Consequently, there is a high probability that the upper part of S<sub>4</sub> has been truncated. Further correlation of susceptibility records from other locations in North Bulgaria (see below) supports this interpretation. The dominant role of the fine grained magnetic fraction in the total magnetic enhancement is demonstrated by the positive relationship between low field susceptibility, frequency dependent susceptibility and the proportion of the fine fraction determined by grain size analysis (Fig. 4).

Palaeoenvironmental changes during the Brunhes chron influenced both rock-magnetic and geochemical characteristics (e.g. CaCO<sub>3</sub>, organic content) as is seen from their correspondence with lithologic boundaries (Fig. 2). According to earlier studies on Bulgarian loess (Minkov 1968; Stoilov 1984) carbonates are inherent to the primary dust material, while the observed stratigraphic variations are mainly due to secondary redistribution as a result of pedogenesis. Meteoric precipitation is very probably the main cause of the redistribution of the calcium carbonate (Jenny 1941; Weaver 1989; Fang *et al.* 1999). The observed increase in CaCO<sub>3</sub> content towards the top of each of the palaeosols S<sub>1</sub>, S<sub>2</sub>, S<sub>3</sub> and S<sub>5</sub> (Fig. 2) is probably the result of secondary carbonate precipitation from the overlying accumulated loesses. For palaeosols S<sub>2</sub> and S<sub>5</sub>, this assumption is supported also by the fact that the overlying loess units, L<sub>2</sub> and L<sub>5</sub>, respectively, are characterized by a relative decrease of the clay fraction ( $d < 0.005$  mm) (Fig. 2), which promotes carbonate leaching down the profile due to water infiltration. From the palaeoclimatic point of view, this suggests that the closing of the warm stages, responsible for the development of palaeosols S<sub>1</sub>, S<sub>2</sub>, S<sub>3</sub> and S<sub>5</sub> were characterized by an increase in mean precipitation. The situation for palaeosol S<sub>6</sub> (Fig. 2) is different. The higher CaCO<sub>3</sub> content throughout the solum suggests a relatively dry climate prevailing during the formation of S<sub>6</sub>. The presence of secondary (neoformed) carbonates in the A horizons of palaeosols in the Viatovo section has also been observed in similar loess/palaeosol sections in the Ukraine (Tsatskin *et al.* 1998). The inverse correlation between magnetic susceptibility ( $\chi$ ) and CaCO<sub>3</sub> (Fig. 2) cannot entirely account for the magnetic enhancement of the palaeosol horizons. As in loess/palaeosol sections in China (Hus & Han 1992; Zhengtang *et al.* 1993; Feng & Johnson 1995), the diamagnetic contribution of CaCO<sub>3</sub> to the dilution of magnetic signal can only account for between 7 and 25 per cent. The relatively high degree of pedogenesis

and weathering in the Viatovo section is probably the reason for the observed small variations in the clay content (Fig. 2). The latter is also evident from the high  $\chi_{FD}$  per cent, which shows low values (e.g. low pedogenic alteration) only in loess units L<sub>2</sub> and L<sub>5</sub>.

The magnetic susceptibility signature of the loess-palaeosol sequence of North Bulgaria was compared with the astronomically tuned marine oxygen isotope records (Shackleton & Hall 1989; Shackleton *et al.* 1990) in order to check the potential of the Viatovo section to reflect global and/or regional palaeoclimate (Fig. 9). In a previous study (Jordanova & Petersen 1999), S<sub>1</sub> was matched to stage 5 of the  $\delta^{18}O$  record. Comparison of the magnetic record of the Viatovo section with other loess/palaeosol records from North Bulgaria (Koriten and Lubenovo, Fig. 9) gives a wider view of the Quaternary climate of the region. A thin loess layer in the thick last interglacial palaeosol complex in the Lubenovo record has been detected (Fig. 9). The very close similarity of all the details of the magnetic susceptibility variations of the three profiles is striking. The incipient palaeosol in unit L<sub>1</sub> is clearly indicated, although the absolute values of susceptibility variations are small. A similar pattern is observed in susceptibility records from loess-palaeosol sequences in Northwestern Bulgaria and the Black Sea (Avramov *et al.* 2006). Magnetic susceptibility behaviour along 21-m-thick loess palaeosol section Mostistea in Romania (Panaiotu *et al.* 2001) shows analogous picture, going to even small details like the exact correspondence of the signal through L<sub>2</sub>–S<sub>2</sub> sequence. The above mentioned sites in Bulgaria and Romania are located at different landscapes along a W–E transect of about 600 km length. Consequently, the major switches in palaeoclimate during the Quaternary are characterized by uniformity of subsequently occurring events, which differ only in their relative intensity. The latter is revealed by significant differences in the degree of relative magnetic susceptibility enhancement of the corresponding palaeosol horizons (Fig. 9). The highest contrast between loess and palaeosol units is observed for the Koriten record, where loess susceptibility is lower than that of the other two records, Viatovo and Lubenovo. It is noteworthy that the latter sections are situated on the Pliocene Denudation Surface (PDS), at an altitude of 165–220 m above sea level in Viatovo in NE Bulgaria and at 242 m in Lubenovo in Central North Bulgaria, higher than the altitude of 70–110 m above sea level at Koriten on the Old Abrasive-Accumulative Level (OAAL) surface (Evlogiev 1993). This difference in altitude may be one of the reasons for the observed variations in loess magnetic susceptibility, as finer and lighter dust material will settle on more elevated terrain, while detrital ferrimagnetic grains are heavier than the silicates of the same size. The role of changing environmental conditions in the source areas due to climate variability during glacial times (Harrison *et al.* 2001) is another possible explanation for quite different background susceptibilities for the different loess horizons (Table 1 and Fig. 3). Differences in the background susceptibility depend also on the degree of post-depositional weathering (e.g. on climate conditions), which obviously is quite significant for the loess layers L<sub>3</sub> and L<sub>7</sub> at Viatovo, taking into account that data points for the two horizons deviate from the obtained positive relationship between  $\chi_{bg}$  and the minimum  $\chi$  in Fig. 3.

## CONCLUSIONS

(1) The loess/palaeosol sequence in Viatovo (North Bulgaria) experienced significant pedogenic alteration, resulting in high amounts of ultrafine grained SP, viscous SP/SD and PSD authigenic magnetite (maghemite) grains in palaeosols but also in older loess horizons.

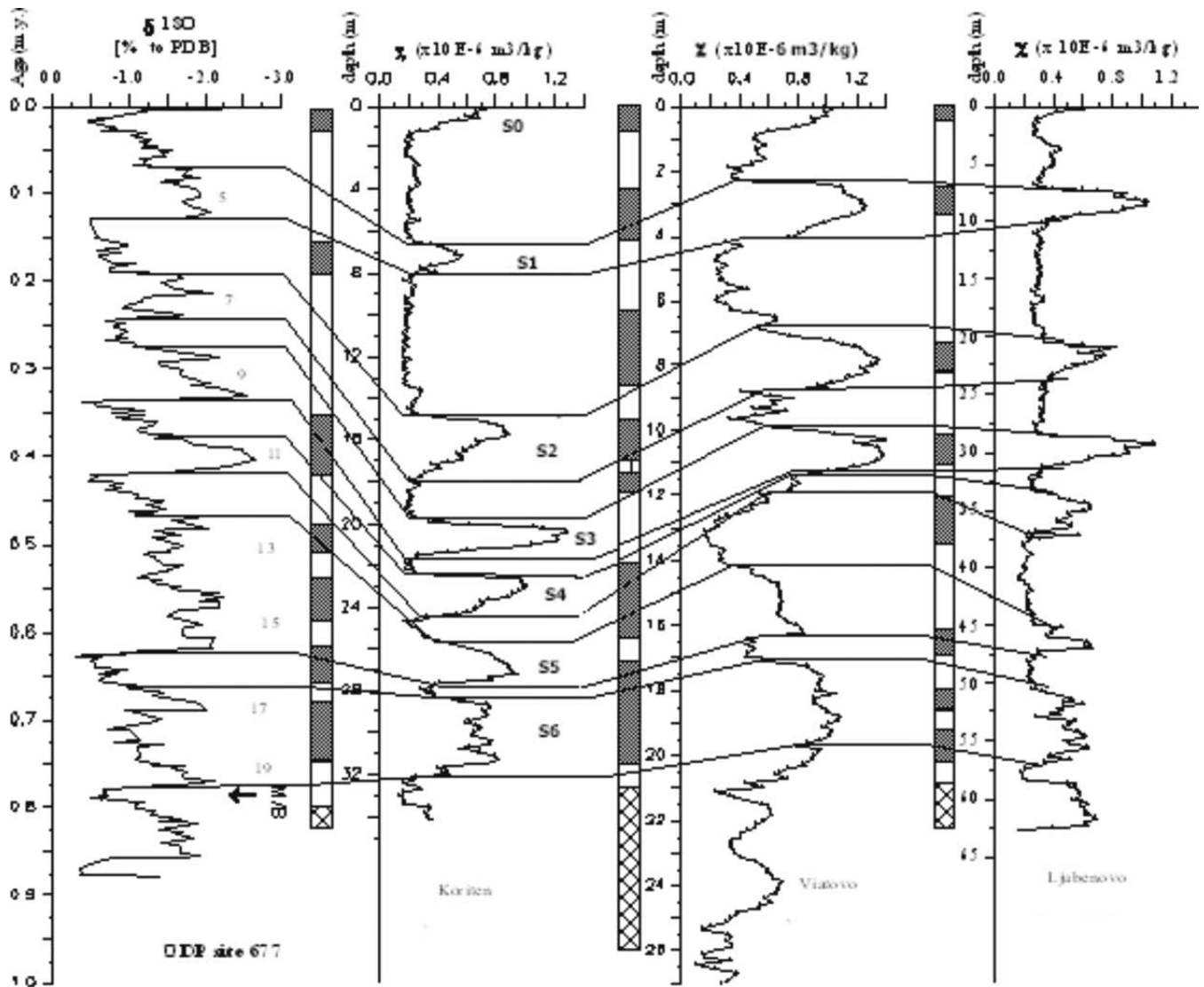


Figure 9. Correlation of the magnetic susceptibility of three loess/palaeosol sequences in Lubenovo (unpublished results), Viatovo and Koriten in Northern Bulgaria (see Fig. 1 for the locations) with the astronomically tuned  $\delta^{18}\text{O}$  record from ODP site 677 of Shackleton and Hall (1989).

(2) Variations of low-field magnetic susceptibility, inversely related to the  $\text{CaCO}_3$  content, along the loess-palaeosol sequence in Viatovo reflect changes in palaeoclimatic conditions during the Quaternary.

(3) Differences in the behaviour of magnetic susceptibility and induced magnetization in stronger fields of loess and palaeosol samples during heating are probably caused by the presence or absence of ferrihydrite and reductants in the material.

(4) There is a remarkable similarity of the magnetic susceptibility signatures of three complete loess/palaeosol sequences along a W–E transect in North Bulgaria, consistent also with the published data for other loess-palaeosol sections in the area. Differences in the relative magnetic enhancement of palaeosol units of the same age suggest differences in palaeoclimatic conditions at a regional scale.

ACKNOWLEDGMENTS

This work was carried out in the framework of bilateral cooperation between the Geophysical Institute of the Bulgarian Academy of Sciences and the Geophysical Centre of the Royal Meteorological

Institute (Dourbes, Belgium). Partial financial support from EMIRA project (No -11/01.09.2005) is also acknowledged.

REFERENCES

Avramov, V., Jordanova, D., Hoffmann, V. & Roesler, W., 2006. The role of dust source area and pedogenesis of three loess-palaeosol sections from North Bulgaria—a mineral magnetic study, *Studia Geophys. Geodaet.*, **50**, 259–282.

Campbell, A., Schwertmann, U. & Campbell, P., 1997. Formation of cubic phases on heating ferrihydrite, *Clay Miner.*, **32**, 615–622.

Chen, T., Xu, H., Xie, Q., Chen, J., Ji, J. & Lu, H., 2005. Characteristics and genesis of maghemite in Chinese loess and palaeosols: mechanism for magnetic susceptibility enhancement in palaeosols, *Earth Planet. Sci. Lett.*, **240**, 790–802.

Cornell R. & Schwertmann, U., 1996. *The Iron Oxides. Structure, Properties, Reactions, Occurrence and Uses*, Weinheim, New York.

Dearing, J., Bird, P., Dann, R. & Benjamin, S., 1997. Secondary ferrimagnetic minerals in Welsh soils: a comparison of mineral magnetic detection methods and implications for mineral formation, *Geophys. J. Int.*, **130**, 727–736.

- Deng, C., Zhu, R., Verosub, K., Singer, M. & Vidic, N., 2004. Mineral magnetic properties of loess/palaeosol couplets of the central loess plateau of China over the last 1.2 Myr, *J. geophys. Res.*, **109**, B01103, doi:10.1029/2003JB002532.
- Deng, C., Vidic, N., Verosub, K., Singer, M., Liu, Q., Shaw, J. & Zhu, R., 2005. Mineral magnetic variation of the Jiaodao Chinese loess/palaeosol sequence and its bearing on long-term climatic variability, *J. geophys. Res.* **110**, B03103, doi:10.1029/2004JB003451.
- Ding, Z.L., Derbyshire E., Yang, S.L., Xu, W., Xiong, S.F. & Liu, T.S., 2002. Stacked 2.6 Ma grain size record from the Chinese loess based on five sections and correlation with the deep-sea 18 $\delta$ O record, *Paleoceanography*, **17**, doi:10.1029/2001PA000725.
- Dunlop D. & Ozdemir, O., 1997. Rock magnetism. Fundamentals and frontiers, in *Cambridge Studies in Magnetism*, ed. Edwards, D., Cambridge University Press, Cambridge, UK.
- Evlogiev, J., 1993. Palaeogeography and stratigraphy of the Early Pleistocene in near Danube Northeastern Bulgaria, PhD thesis, Bulgarian Academy of Sciences, Sofia, (in Bulgarian).
- Evlogiev, J., 2006. The Pleistocene and Holocene in the Danube plain, *Doctoral dissertation, Bulg. Acad. Sci.* (in Bulgarian).
- Eyre, J. & Shaw, J., 1994. Magnetic enhancement of Chinese loess—the role of  $\gamma$ Fe<sub>2</sub>O<sub>3</sub>? *Geophys. J. Int.*, **117**, 265–271.
- Fang, X. *et al.*, Asian summer monsoon instability during the past 60 000 years: magnetic susceptibility and pedogenic evidence from the western Chinese Loess Plateau, *Earth Planet. Sci. Lett.*, **168**, (1999) 219–232.
- Feng Z.-D. & Johnson, W., 1995. Factors affecting the magnetic susceptibility of loess-soil sequence, Barton County, Kansas, USA, *Catena*, **24**, 25–37.
- Forster T. & Heller, F., 1997. Magnetic enhancement paths in loess sediments from Tajikistan, China and Hungary, *Geophys. Res. Lett.*, **24**, 17–20.
- Forster, T., Evans, M. & Heller, F., 1994. The frequency dependence of low field magnetic susceptibility in loess sediments, *Geophys. J. Int.*, **118**, 636–642.
- Gehring, A. & Hofmeister, A., 1994. The transformation of lepidocrocite during heating: a magnetic and spectroscopic study, *Clays Clay Miner.*, **42** (No. 4), 409–415.
- Goodman, B., 1994. Mossbauer spectroscopy of oxide minerals, in *Clay Mineralogy: Spectroscopic and Chemical Determinative Methods*, pp. 82–96, ed. M. Wilson, Chapman and Hall, London.
- Harrison, S., Kohfeld, K., Roelandt, C. & Claquin, T., 2001. The role of dust in climate changes today, at the last glacial maximum and in the future, *Earth Sci. Rev.* **54**, 43–80.
- Heller, F. & Evans, M., 1995. Loess magnetism, *Rev. Geophys.*, **33**(2), 211–240.
- Heller, F. Xiuming, L. Tungsheng, L. & Tongchun, X., 1991. Magnetic susceptibility of loess in China, *Earth Planet. Sci. Lett.*, **103**, 301–310.
- Hus, J. & Han, J., 1992. The contribution of loess magnetism in China to the retrieval of past global changes—some problems, *Phys. Earth Planet. Inter.*, **70**, 154–168.
- Jenny, H., 1941. Factors of soil formation, in *A System of Quantitative Pedology*, R. Amundson, Dover Publ. Inc., New York (edition 1994).
- Jordanova D. & Petersen, N., 1999a. Palaeoclimatic record from a loess-soil profile in northeastern Bulgaria – I. Rock magnetic properties, *Geophys. J. Int.* **138** (2), 520–532.
- Jordanova D. & Petersen, N., 1999b. Palaeoclimatic record from a loess-soil profile in northeast Bulgaria – II. Correlation with global climatic events during the Pleistocene, *Geophys. J. Int.*, **138** (2), 533–540.
- Liu, Q., Banerjee, S., Jackson, M., Deng, Ch., Pan, Y. & Zhu, R., 2004. New insights into partial oxidation model of magnetites and thermal alteration of magnetic mineralogy of the Chinese loess in air, *Geophys. J. Int.*, **158**, 506–514.
- Liu, Q., Banerjee, S. K., Jackson, M., Maher, B., Pan, Y., Zhu, R., Deng, Ch. & Chen, F., 2004a. Grain sizes of susceptibility and anhysteretic remanent magnetization carriers in Chinese loess/palaeosol sequences, *J. geophys. Res.* **109**, B03101, doi:10.1029/2003JB002747.
- Liu, Q., Jackson, M., Banerjee, S., Maher, B., Deng, Ch., Pan, Y. & Zhu, R., 2004b. Mechanism of the magnetic susceptibility enhancements of the Chinese loess, *J. geophys. Res.*, **109**, B12107, doi:10.1029/2004JB003249.
- Maher, B., 1986. Characterization of soils by mineral magnetic measurements, *Phys. Earth Planet. Inter.*, **42**, 76–92.
- Maher, B., 1988. Magnetic properties of modern soils and Quaternary loessic paleosols: paleoclimatic implications, *Palaeogeogr. Palaeoclimat. Palaeoecol.*, **137**, 25–54.
- Maher, B., 1998. Magnetic properties of modern soils and Quaternary loessic paleosols: paleoclimatic implications, *Palaeogeogr. Palaeoclimat. Palaeoecol.* **137**, 25–54.
- Maher B. & Thompson, R., 1992. Paleoclimatic significance of the mineral magnetic record of the Chinese loess and paleosols, *Quart. Res.*, **37**, 155–170.
- Maher, B. & Thompson, R., 1995. Paleorainfall reconstructions from pedogenic magnetic susceptibility variations in the Chinese loess and paleosols, *Quat. Res.*, **44**, 383–391.
- Maher, B., Thompson, R. & Zhou, L.-P., 1994. Spatial and temporal reconstructions of changes in the Asian palaeomonsoon: a new mineral magnetic approach, *Earth Planet. Sci. Lett.*, **125**, 462–471.
- Minkov, M., 1968. *Loess in North Bulgaria*, Bulgarian Academy of Sciences, Sofia (in Bulgarian).
- Mullins, C., 1977. Magnetic susceptibility of the soil and its significance in soil science—a review, *J. Soil Sci.*, **28**, 223–246.
- Murad, E., 1998. Clays and clay minerals: what can Mossbauer spectroscopy do to help understand them? *Hyperfine Interact.*, **117**, 39–70.
- Murad E. & Wagner, U., 1998. Clays and clay minerals: the firing process, *Hyperfine Interact.*, **117**, 337–356.
- Oches E. & Banerjee, S.K., 1996. Rock-magnetic proxies of climate change from loess-paleosol sediments of the Czech Republic, *Stud. Geophys. Geodaet.*, **40**, 287–301.
- O'Reilly, 1984. *Rock and Mineral Magnetism*. Blackie, Chapman and Hall, Glasgow and London, UK.
- Ozdemir O. & Dunlop, D., 1993. Chemical remanent magnetization during gamma FeOOH phase transformations, *J. Geophys. Res.*, **98**, 4191–4198.
- Panaiotu, C., Panaiotu E., Grama, A. & Necula, C., 2001. Paleoclimatic record from loess-paleosol profile in Southeastern Romania, *Phys. Chem. Earth (A)*, **26**, 893–898.
- Qiu, X., Cai B. & Liu, T., 2005. Loess record of the aerodynamic environment in the east Asia monsoon area since 60 000 years before present, *J. geophys. Res.* **110**, B01204, doi:10.1029/2004JB003131.
- Shackleton, N. & Hall, M., 1989. Stable isotope history of the Pleistocene at ODP site 677, *Proc. Ocean Drilling Program, Scientific Results*, **111**, 295–316.
- Shackleton, N., Berger A. & Peltier, R., 1990. An alternative astronomical calibration of the lower Pleistocene timescale based on ODP site 677, *Trans. R. Soc. Edinburg Earth Sci.*, **81**, 251–261.
- Schwertmann, U., 1988. Occurrence and formation of iron oxides in various pedoenvironments, in *Iron in Soils and Clay Minerals*, Vol.217, pp. 267–308, eds Stucki, J.; Goodman, B. & Schwertmann, U., NATO ASI Series, Series C: Mathematical and Physical Sciences, Reidel Publ. Company, Dordrecht, Holland.
- Stoilov, K., 1984. *Loess Formation in Bulgaria*. Bulgarian Academy of Sciences, Sofia (in Bulgarian).
- Sun, Y.B. & An, Z.S., 2004. An improved comparison of Chinese loess with deep-sea 18 $\delta$ O record over the interval 1.6–2.6 Ma, *Geophys. Res. Lett.*, **31**, doi:10.1029/2004GL019716.
- Tsatskin, A., Heller, F., Hailwood, E., Gendler, T., Hus, J., Montgomery, P., Sartori, M. & Virina, E., 1998. Pedosedimentary division, rock magnetism and chronology of the loess/palaeosol sequence at Roxolany (Ukraine), *Palaeogeogr. Palaeoclimat. Palaeoecol.*, **143**, 111–133.
- Turin, I., 1937. *Organic Matter in Soils and its Role for Pedogenesis and Soil Fertility*. Selhooziz, Leningrad, pp. 286 (in Russian).
- Vandenbergh, R., De Grave, E., Landuydt C. & Bowen, L. H., 1990. Some aspects concerning the characterization of iron oxides and hydroxides in soils and clays, *Hyperfine Interact.*, **53**, 175–196.

- Van Velzen, A. & Dekkers, M., 1999. The incorporation of thermal methods in mineral magnetism of loess-palaeosol sequences: a brief overview, *Chin. Sci. Bull.* **44**, 53–63.
- Weaver, C., 1989. *Clays, Muds and Shales. Developments in Sedimentology*, Vol. 44, Elsevier, Amsterdam-Oxford-New York-Tokyo.
- Wells, M., Fitzpatrick, R., Gilkes, R. & Dobson, J., 1999. Magnetic properties of metal-substituted haematite. *Geophys. J. Int.*, **138**, 571–580.
- Zhengtang, G., Fedoroff, N., Zhisheng, A. & Liu, T., 1993. Inter-glacial dustfall and origin of iron oxides-hydroxides in the palaeosols of the Xifeng loess section, China. *Sci. Geol. Sin.*, **2** (1), 91–100.
- Zhou, L.P., Oldfield, F.A., Wintle, G., Robinson, S.G. & Wang, J.J., 1990. Partly pedogenic origin of magnetic variations in Chinese loess. *Nature*, **346**, 737–739.